

1 Measurement of the Bottom-Strange Meson Mixing
2 Phase in the Full CDF Data Set

3 The CDF Collaboration

4 August 9, 2012

5 **Abstract**

6 We report a measurement of the bottom-strange meson mixing
7 phase β_s using the time evolution of $B_s^0 \rightarrow J/\psi(\rightarrow \mu^+ \mu^-) \phi(\rightarrow K^+ K^-)$
8 decays in which the quark-flavor content of the bottom-strange meson
9 is identified at production. This measurement uses the full data set of
10 proton-antiproton collisions at $\sqrt{s} = 1.96$ TeV collected by the Col-
11 lider Detector experiment at the Fermilab Tevatron, corresponding to
12 9.6 fb^{-1} of integrated luminosity. We report confidence regions in the
13 two-dimensional space of β_s and the B_s^0 decay-width difference $\Delta\Gamma_s$,
14 and measure $\beta_s \in [-\pi/2, -1.51] \cup [-0.06, 0.30] \cup [1.26, \pi/2]$ at the
15 68% confidence level, in agreement with the standard model expect-
16 ation. Assuming the standard model value of β_s , we also determine
17 $\Delta\Gamma_s = 0.068 \pm 0.026(\text{stat}) \pm 0.009(\text{syst}) \text{ ps}^{-1}$ and the mean B_s^0 life-
18 time, $\tau_s = 1.528 \pm 0.019(\text{stat}) \pm 0.009(\text{syst}) \text{ ps}$, which are consistent
19 and competitive with determinations by other experiments.

1 The noninvariance of the physics laws under the simultaneous transfor-
 2 mations of parity and charge conjugation (CP violation) is accommodated in
 3 the standard model (SM) through the presence of a single irreducible complex
 4 phase in the weak-interaction couplings of quarks. A broad class of generic
 5 extensions of the SM is expected to naturally introduce additional sources of
 6 CP violation that should be observable, making CP -violation studies promis-
 7 ing to search for experimental indications of new particles or interactions.
 8 Thus far, CP violation has been established in transitions of strange and
 9 bottom hadrons, with effects consistent with the SM interpretation [1, 2, 3].
 10 Much less information is available for bottom-strange mesons, B_s^0 . Studies
 11 of $B_s^0-\bar{B}_s^0$ flavor oscillations are unique in that they probe the quark-mixing
 12 (Cabibbo-Kobayashi-Maskawa, CKM) matrix element V_{ts} , which directly en-
 13 ters the mixing amplitude. Large non-SM enhancements of the mixing am-
 14 plitude are excluded by the precise determination of the oscillation frequency
 15 in 2006 [4]. However, non-SM particles or couplings involved in the mixing
 16 may also increase the size of the observed CP violation by enhancing the
 17 mixing phase $\beta_s = \arg[-(V_{ts}V_{tb}^*)/(V_{cs}V_{cb}^*)]$ [5] with respect to the value ex-
 18 pected from the CKM hierarchy, $\beta_s^{\text{SM}} \approx 0.02$ [2], henceforth referred to as
 19 ‘SM expectation’. A non-SM enhancement of β_s would also decrease the size
 20 of the decay-width difference between the light and heavy mass eigenstates
 21 of the B_s^0 meson, $\Delta\Gamma_s = \Gamma_L - \Gamma_H$. The values of the mixing phase and width
 22 difference are loosely constrained, and currently the subject of intense ex-
 23 perimental activity. The analysis of the time evolution of $B_s^0 \rightarrow J/\psi\phi$ decays

1 provides the most effective determination of β_s and $\Delta\Gamma_s$ [6]. Assuming neg-
2 ligible contributions from sub-leading decay amplitudes [7], the underlying
3 $b \rightarrow c\bar{c}s$ quark transition is dominated by a single real amplitude, making β_s
4 the sole CP -violating phase observable, through the interference between the
5 amplitudes of decays occurring with and without oscillations.

6 The first determinations of β_s , by the CDF and D0 experiments, suggested
7 a mild deviation from the SM expectation [8]. The interest in this measure-
8 ment increased further recently, because of the 3.9σ departure from the SM
9 expectation of the dimuon asymmetry observed by D0 in semileptonic decays
10 of $B_{(s)}^0$ mesons [9], which is tightly correlated with β_s , if generated in the B_s^0
11 sector [5]. While updated measurements in $B_s^0 \rightarrow J/\psi\phi$ decays [10, 11, 12, 13]
12 showed increased consistency with the SM, more precise experimental infor-
13 mation is needed for a conclusive interpretation.

14 In this Letter we report a measurement of β_s ; $\Delta\Gamma_s$; the mean lifetime
15 of heavy and light B_s^0 mass eigenstates, $\tau_s = 2/(\Gamma_H + \Gamma_L)$; and the an-
16 gular momentum composition of the signal sample using the final data set
17 collected by the CDF experiment at the Tevatron proton-antiproton col-
18 lider, corresponding to an integrated luminosity of 9.6 fb^{-1} . The analysis
19 closely follows a previous measurement from a subset of the present data
20 [10], and introduces an improved determination of the sample composition
21 based on a new study of the K^+K^- and $J/\psi K^+K^-$ mass distributions. The
22 CDF II detector is a magnetic spectrometer surrounded by electromagnetic
23 and hadronic calorimeters and muon detectors that has cylindrical geome-

1 try with forward-backward symmetry. Charged particle trajectories (tracks)
 2 are reconstructed using single- and double-sided silicon microstrip sensors
 3 arranged in seven cylindrical layers [14] and an open cell drift chamber with
 4 96 layers of sense wires [15], all immersed in a 1.4 T axial magnetic field.
 5 The resolution on the momentum component transverse to the beam, p_T ,
 6 is $\sigma_{p_T}/p_T^2 \approx 0.07\%$ (p_T in GeV/ c), corresponding to a mass resolution of
 7 our signals of about 9 MeV/ c^2 . Muons with $p_T > 1.5$ GeV/ c are detected
 8 in multiwire drift chambers [16]. A time-of-flight detector identifies charged
 9 particles with $p_T < 2$ GeV/ c [17], complemented by the ionization-energy-loss
 10 measurement in the drift chamber at higher transverse momenta. The com-
 11 bined identification performance corresponds to a separation between charged
 12 kaons and pions of approximately two Gaussian standard deviations, nearly
 13 constant in the relevant momentum range. Events enriched in $J/\psi \rightarrow \mu^+ \mu^-$
 14 decays are recorded using a low- p_T dimuon online selection (trigger) that
 15 requires two oppositely-charged particles reconstructed in the drift chamber
 16 matched to muon chamber track segments, with a dimuon mass between 2.7
 17 and 4.0 GeV/ c^2 .

18 In the analysis, two tracks matched to muon pairs are required to be
 19 consistent with a $J/\psi \rightarrow \mu^+ \mu^-$ decay, with dimuon mass $3.04 < m_{\mu\mu} < 3.14$
 20 GeV/ c^2 . These are combined with another pair of tracks consistent with a
 21 $\phi \rightarrow K^+ K^-$ decay, $1.009 < m_{KK} < 1.028$ GeV/ c^2 , in a kinematic fit to a com-
 22 mon vertex. A dimuon mass constraint to the known J/ψ mass [1] improves
 23 the B_s^0 mass resolution. An artificial neural network (NN) classifier [10] com-

1 bins multiple discriminating variables into a single quantity that statistically
 2 separates the signal from the dominant background from combinations of real
 3 J/ψ decays with random track pairs and a minor component of random four-
 4 track combinations (both collectively referred to as combinatorics). The NN
 5 is trained with simulated events for the signal and data from sidebands in
 6 B_s^0 mass, $[5.29, 5.31] \cup [5.42, 5.45]$ GeV/ c^2 , for the background. In decreasing
 7 order of discriminating power, the input variables to the NN include kine-
 8 matic quantities, muon and hadron particle identification information, and
 9 vertex fit quality parameters.

10 Figure 1 shows the $J/\psi K^+ K^-$ mass distribution from the final sample of
 11 candidates that pass an NN threshold chosen as to maximize the sensitivity to
 12 the measurement of β_s [10]. The distribution shows a signal of approximately
 13 11 000 decays, above a fairly constant background dominated by the prompt
 14 combinatorial component, and smaller contributions from mis-reconstructed
 15 B decays.

16 We determine the quantities of interest using a fit to the time evolution
 17 of bottom-strange mesons. The differences in time evolution of states ini-
 18 tially produced as a B_s^0 or \bar{B}_s^0 meson are included in the fit as well as the
 19 differences between decays that result in a CP -odd or CP -even combination
 20 of the $J/\psi\phi$ angular momenta. The proper decay time of a B_s^0 candidate is a
 21 fit observable calculated as $t = ML_{xy}/p_T$, where L_{xy} is the distance from the
 22 primary vertex to the B_s^0 decay vertex, projected onto the B_s^0 momentum
 23 in the plane transverse to the beam, \vec{p}_T ; and M is the known mass of the

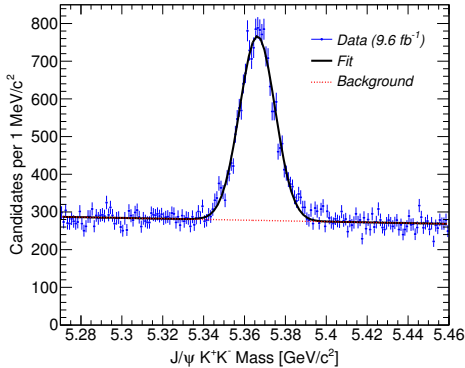


Figure 1: (Color online) Distribution of $J/\psi K^+ K^-$ mass with fit projection overlaid.

1 B_s^0 meson [1]. The proper decay-time uncertainty, σ_t , is calculated from the
 2 measurement uncertainties in L_{xy} . Because the B_s^0 meson has spin zero and
 3 J/ψ and ϕ have spin one, the $B_s^0 \rightarrow J/\psi \phi$ decay involves three possible an-
 4 gular momentum states of the $J/\psi \phi$ system. These are combined into three
 5 polarization amplitudes, longitudinal polarization (A_0), and transverse po-
 6 larization with spins parallel (A_{\parallel}) or perpendicular (A_{\perp}) to each other. The
 7 first two states are CP even, while the last one is CP odd. A CP -odd state
 8 can also be produced by a nonresonant $K^+ K^-$ pair or can originate from
 9 the decay of the spin-0 $f_0(980)$ meson, which results in another independent
 10 decay amplitude, the S -wave A_S .

11 To enhance the sensitivity to β_s , the time-evolution of the four decay am-
 12 plitudes along with six interference terms is fitted simultaneously by exploit-
 13 ing differences in the distribution of the kaons' and muons' decay angles. The
 14 angles are parametrized in the transversity basis, $\vec{\rho} = (\cos \Theta, \Phi, \cos \Psi)$ [18],

1 which allows a convenient separation of the CP -even and CP -odd terms
 2 in the likelihood. Reference [19] details the expression for the decay rate
 3 differential in the decay time and angles. The rate is a function of the
 4 physics parameters of interest, β_s , $\Delta\Gamma_s$, τ_s , and the decay amplitudes with
 5 their CP -conserving phases. For these we choose A_0 to be real and de-
 6 fine the CP -conserving phases as $\delta_{\parallel} = \arg(A_{\parallel}/A_0)$, $\delta_{\perp} = \arg(A_{\perp}/A_0)$ and
 7 $\delta_S = \arg(A_S/A_0)$. The decay rate is also a function of the B_s^0 mixing fre-
 8 quency, which is a fit parameter constrained to the experimental value mea-
 9 sured by CDF, $\Delta m_s = 17.77 \pm 0.12 \text{ ps}^{-1}$ [4].

10 The flavor of the meson at the time of production is inferred by two
 11 independent classes of flavor tagging algorithms [10], which exploit specific
 12 features of the incoherent production of $b\bar{b}$ quarks-pairs in $p\bar{p}$ collisions. Us-
 13 ing flavor conservation of the strong interaction, the opposite-side flavor tag
 14 (OST) infers the signal production flavor from the decay products of the
 15 b hadron produced by the other b quark in the event by using the charge
 16 of muons or electrons from semileptonic B decays or the net charge of the
 17 opposite-side jet. The same-side kaon tag (SSKT) deduces the signal produc-
 18 tion flavor by exploiting charge-flavor correlations of the neighboring kaons
 19 produced during its fragmentation. The fraction of candidates tagged by a
 20 combination of OST algorithms totals $\varepsilon_{\text{OST}} = (92.8 \pm 0.1)\%$. The probability
 21 of wrongly-tagging the meson, w_{OST} , is determined per event and calibrated
 22 using 82 000 $B^{\pm} \rightarrow J/\psi(\rightarrow \mu^+ \mu^-) K^{\pm}$ decays fully reconstructed in the same
 23 sample as the signal [20]. Because the B^{\pm} does not oscillate, the OST tag

1 is compared with the actual flavor, known from the charge of the K^\pm me-
 2 son. A single scale factor that matches the predicted mistag probability to
 3 the one observed in data is then extracted. The observed averaged dilution,
 4 $D_{\text{OST}} = 1 - 2w_{\text{OST}}$, equals $(12.3 \pm 0.6)\%$, resulting in a tagging power of
 5 $\varepsilon_{\text{OST}} D_{\text{OST}}^2 = (1.39 \pm 0.05)\%$. The SSKT algorithms tag a smaller fraction of
 6 candidates, $\varepsilon_{\text{SSKT}} = (52.2 \pm 0.7)\%$, with better precision. A $(21.8 \pm 0.3)\%$
 7 dilution has been obtained by measuring the B_s^0 mixing frequency in ap-
 8 proximately 11 000 (1 850) $B_s^0 \rightarrow D_s^- \pi^+ (\pi^+ \pi^-)$ decays reconstructed in the
 9 data corresponding to the first 5.2 fb^{-1} [10]. The SSKT tagging power is
 10 $(3.2 \pm 1.4)\%$ in that sample. Higher instantaneous luminosity conditions in
 11 later data resulted in a reduced trigger efficiency for hadronic B_s^0 decays.
 12 Hence, the additional sample of $B_s^0 \rightarrow D_s^- \pi^+ (\pi^+ \pi^-)$ decays is too limited for
 13 a significant test of the SSKT performance. Because the SSKT calibration
 14 is known for early data only, we conservatively restrict its use to the events
 15 collected in that period. Simulation shows that this results in a degradation
 16 in β_s resolution not exceeding 15%.

17 The unbinned maximum likelihood fit uses 9 observables from each event
 18 to determine 32 parameters including β_s and $\Delta\Gamma$, other physics parameters
 19 such as B_s^0 lifetime, amplitudes and phases, and several other quantities,
 20 called *nuisance* parameters, such as tagging dilution scale factors. The fit
 21 uses the information of the reconstructed B_s^0 candidate mass and its uncer-
 22 tainty, m and σ_m ; the B_s^0 candidate proper decay time and its uncertainty,
 23 t and σ_t ; the transversity angles, $\vec{\rho}$; and tag information, \mathcal{D} and ξ ; where

1 \mathcal{D} is the event-specific dilution given by the mistag probability, and ξ is the
 2 tag decision. Both tagged and untagged events are used in the fit. The
 3 single-event likelihood is described in terms of signal, P_s , and background,
 4 P_b , probability density functions (density henceforth) as

$$\begin{aligned} \mathcal{L} &\propto f_s P_s(m|\sigma_m) P_s(t, \vec{\rho}, \xi | \mathcal{D}, \sigma_t) P_s(\sigma_t) P_s(\mathcal{D}) \\ &+ (1 - f_s) P_b(m) P_b(t|\sigma_t) P_b(\vec{\rho}) P_b(\sigma_t) P_b(\mathcal{D}), \end{aligned} \quad (1)$$

5 where f_s is the fraction of signal events. The signal mass density $P_s(m|\sigma_m)$ is
 6 parametrized as a single Gaussian with a width determined independently for
 7 each candidate. The background mass density, $P_b(m)$, is parametrized as a
 8 straight line. The time and angular dependence of the signal, $P_s(t, \vec{\rho}, \xi, | \mathcal{D}, \sigma_t)$,
 9 for a single flavor tag are written in terms of two densities, P for B_s^0 and \bar{P}
 10 for \bar{B}_s^0 , as

$$\left(\frac{1 + \xi \mathcal{D}}{2} P(t, \vec{\rho} | \sigma_t) + \frac{1 - \xi \mathcal{D}}{2} \bar{P}(t, \vec{\rho} | \sigma_t) \right) \varepsilon(\vec{\rho}), \quad (2)$$

11 which is extended to the case of OST and SSKT independent flavor tags.
 12 Acceptance effects on the transversity angle distributions are modeled with
 13 an empirical three-dimensional joint probability density function extracted
 14 from simulation, $\varepsilon(\vec{\rho})$. The time and angular distributions for flavor-tagged
 15 B_s^0 (\bar{B}_s^0) decays, P (\bar{P}), are given by the normalized decay rate as functions of
 16 decay time and transversity angles of Ref. [19], assuming no CP violation in
 17 the decay. Building on previous measurements [21], we model the decay-time
 18 density for the background, $P_b(t|\sigma_t)$, with a δ -function at $t = 0$, one posi-

1 tive, and two negative exponential functions. All time-dependent terms are
 2 convolved with a proper time resolution function, modeled as a sum of two
 3 Gaussians with common mean and independent widths determined by the
 4 fit. The resulting decay-time resolution is equivalent to that of a Gaussian
 5 distribution with 90 fs standard deviation. The background angular proba-
 6 bility density, factorized as $P_b(\vec{\rho}) = P_b(\cos \Theta)P_b(\Phi)P_b(\cos \Psi)$, is determined
 7 from B_s^0 mass sideband events. The distributions of the decay-time uncer-
 8 tainty and the event-specific dilution differ for signal and background events,
 9 thus their densities are explicitly included in the likelihood. The probability
 10 density functions of the decay-time uncertainties, $P_s(\sigma_t)$ and $P_b(\sigma_t)$, are de-
 11 scribed with an empirical model from an independent fit to the data. The sig-
 12 nal density, $P_s(\mathcal{D})$, is determined from binned background-subtracted signal
 13 distributions, while the background density, $P_b(\mathcal{D})$, is modeled from candi-
 14 dates in the signal sidebands. Potential sources of systematic uncertainties,
 15 associated with imprecisely known calibration factors of tagging dilutions,
 16 are taken into account by floating these factors in the fit within Gaussian
 17 constraints.

The likelihood function shows two equivalent global maxima, correspond-
 ing to the solutions with positive and negative value of $\Delta\Gamma_s$, and additional
 local maxima generated by approximate symmetries [19]. Multiple solutions
 make the estimation of parameters and their uncertainties challenging with
 limited sample size. If β_s is fixed to its SM value, the fit shows unbiased
 estimates and Gaussian uncertainties for $\Delta\Gamma_s$, τ_s , polarization amplitudes,

and the phase δ_{\perp} , yielding

$$\begin{aligned}\tau_s &= 1.528 \pm 0.019(\text{stat}) \pm 0.009(\text{syst}) \text{ ps}, \\ \Delta\Gamma_s &= 0.068 \pm 0.026(\text{stat}) \pm 0.009(\text{syst}) \text{ ps}^{-1}, \\ |A_0|^2 &= 0.512 \pm 0.012(\text{stat}) \pm 0.018(\text{syst}), \\ |A_{\parallel}|^2 &= 0.229 \pm 0.010(\text{stat}) \pm 0.014(\text{syst}), \\ \delta_{\perp} &= 2.79 \pm 0.53(\text{stat}) \pm 0.15(\text{syst}).\end{aligned}$$

1 The correlation between τ_s and $\Delta\Gamma_s$ is 0.52. We do not report a measure-
 2 ment of δ_{\parallel} . The fit determines $\delta_{\parallel} \approx \pi$, but the estimate is biased and
 3 its uncertainty is non-Gaussian because the likelihood symmetry under the
 4 $\delta_{\parallel} \rightarrow 2\pi - \delta_{\parallel}$ transformation [19] results in multiple maxima in the vicin-
 5 ity of $\delta_{\parallel} = \pi$. Systematic uncertainties include mismodeling of the signal
 6 mass model, decay-time resolution, acceptance description, and angular dis-
 7 tribution of the background; an 8% contamination by $B^0 \rightarrow J/\psi K^*(892)^0$
 8 and $B^0 \rightarrow J/\psi K^+ \pi^-$ decays misreconstructed as $B_s^0 \rightarrow J/\psi \phi$ decays; and sil-
 9 icon detector misalignment. For each source, uncertainties are determined
 10 by comparing the fit results from simulated samples in which the systematic
 11 effect is introduced in the model and samples simulated according to the de-
 12 fault model. The uncertainty on the $\Delta\Gamma_s$ measurement is dominated by the
 13 mismodeling of the background decay time. The largest contribution to the
 14 uncertainty on τ_s is the effect of silicon detector misalignment. The angular
 15 acceptance model dominates the systematic uncertainties on the amplitudes.

1 If β_s is free to float in the fit, tests in statistical trials show that the
 2 maximum likelihood estimate is biased for the parameters of interest, and
 3 the biases depend on the true values of the parameters. Hence, we determine
 4 confidence regions in the β_s and $(\beta_s, \Delta\Gamma_s)$ spaces by using a profile-likelihood
 5 ratio statistic as a χ^2 variable and considering all other likelihood variables
 6 as nuisance parameters. The profile-likelihood ratio distributions observed
 7 in simulations deviate from the expected χ^2 distribution, yielding confidence
 8 regions that contain the true values of the parameters with lower proba-
 9 bility than the nominal confidence level. In addition, the profile-likelihood
 10 ratio distribution depends on the true values of the unknown nuisance pa-
 11 rameters. We use a large number of statistical trials to derive the profile-
 12 likelihood ratio distribution of our data. The effect of nuisance parameters
 13 is accounted for by randomly sampling their 30-dimensional space within 5σ
 14 of their estimates in data and using the most conservative of the resulting
 15 profile-likelihood ratio distributions to derive the final confidence regions.
 16 This procedure ensures that the confidence regions have nominal statistical
 17 coverage whatever the configuration of nuisance parameters values and in-
 18 creases the size of the β_s confidence interval by about 40%. We determine
 19 the confidence level for 32×48 evenly spaced points in $\beta_s \in [-\pi/2, \pi/2]$ and
 20 $\Delta\Gamma_s \in [-0.3, 0.3] \text{ ps}^{-1}$ and smoothly interpolate between them to obtain a
 21 continuous region (Fig. 2). Assuming the standard model values for β_s and
 22 $\Delta\Gamma_s$, the probability to observe a profile-likelihood ratio equal to or higher
 23 than observed in data is 54%. By treating $\Delta\Gamma_s$ as a nuisance parameter, we

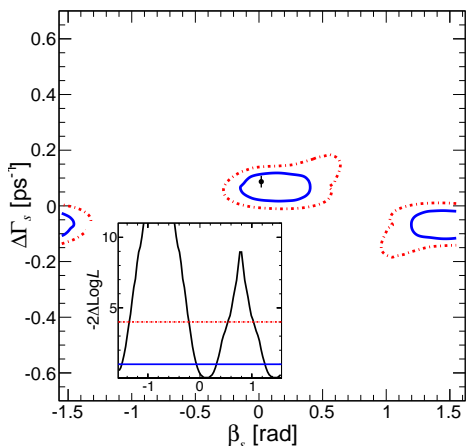


Figure 2: (Color online) Confidence regions at the 68% (solid) and 95% C.L.(dashed) in the $(\beta_s, \Delta\Gamma_s)$ plane (main panel). The standard model prediction is shown as a circle with error bars [22]. The inset shows the coverage-corrected profile-likelihood ratio as a function of β_s , in which $\Delta\Gamma_s$ is treated as all other nuisance parameters.

- 1 also obtain $\beta_s \in [-\pi/2, -1.51] \cup [-0.06, 0.30] \cup [1.26, \pi/2]$ at the 68% C.L.,
- 2 and $\beta_s \in [-\pi/2, -1.36] \cup [-0.21, 0.53] \cup [1.04, \pi/2]$ at the 95% C.L. The
- 3 fraction of S -wave in the K^+K^- mass range 1.009–1.028 GeV/c^2 is deter-
- 4 mined from the angular information to be consistent with zero with $\mathcal{O}(2\%)$
- 5 uncertainty, which is in agreement with our previous determination [10] and
- 6 the LHCb and ATLAS results [12, 13], and inconsistent with the D0 deter-
- 7 mination [11]. An auxiliary simultaneous fit of the K^+K^- and $J/\psi K^+K^-$
- 8 mass distributions [23], which includes the full resonance structure of the
- 9 $B^0 \rightarrow J/\psi K^+ \pi^-$ decay [24], determines a $(0.8 \pm 0.2(\text{stat}))\%$ K^+K^- S -wave
- 10 contribution, in agreement with the central fit. The contamination from mis-
- 11 identified B^0 decays is $(8.0 \pm 0.2(\text{stat}))\%$, which is significantly larger than the

1 1–2% values typically derived assuming only P -wave B^0 decays [10, 11]. If
2 neglected, this additional B^0 component could mimic a larger K^+K^- S -wave
3 than present.

4 In summary we report the final CDF results on the B_s^0 mixing phase and
5 decay width difference from the time-evolution of flavor-tagged $B_s^0 \rightarrow J/\psi\phi$
6 decays reconstructed in the full Tevatron Run II data set. This analysis im-
7 proves and supersedes the previous CDF measurement obtained in a subset
8 of the present data [10]. Considering $\Delta\Gamma_s$ as a nuisance parameter, and using
9 the recent determination of the sign of $\Delta\Gamma_s$ [25], we find $-0.06 < \beta_s < 0.30$
10 at the 68% C.L. Assuming a SM value for β_s , we also report precise mea-
11 surements of decay-width difference, $\Delta\Gamma_s = 0.068 \pm 0.026(\text{stat}) \pm 0.009(\text{syst})$
12 ps^{-1} , and mean B_s^0 lifetime, $\tau_s = 1.528 \pm 0.019(\text{stat}) \pm 0.009(\text{syst})$ ps. All
13 results are consistent with expectations and with determinations of the same
14 quantities from other experiments [11, 12, 13], and significantly improve the
15 knowledge of the phenomenology on CP violation in B_s^0 mixing. We
16 thank the Fermilab staff and the technical staffs of the participating insti-
17 tutions for their vital contributions. This work was supported by the U.S.
18 Department of Energy and National Science Foundation; the Italian Istituto
19 Nazionale di Fisica Nucleare; the Ministry of Education, Culture, Sports,
20 Science and Technology of Japan; the Natural Sciences and Engineering Re-
21 search Council of Canada; the National Science Council of the Republic of
22 China; the Swiss National Science Foundation; the A.P. Sloan Foundation;
23 the Bundesministerium für Bildung und Forschung, Germany; the Korean

1 World Class University Program, the National Research Foundation of Ko-
2 rea; the Science and Technology Facilities Council and the Royal Society,
3 UK; the Russian Foundation for Basic Research; the Ministerio de Cien-
4 cia e Innovación, and Programa Consolider-Ingenio 2010, Spain; the Slovak
5 R&D Agency; the Academy of Finland; and the Australian Research Council
6 (ARC).

7 **References**

8 [1] J. Beringer *et al.* (Particle Data Group), Phys. Rev. D **86**, 010001
9 (2012).

10 [2] Y. Amhis *et al.* (Heavy Flavor Averaging Group), arXiv:1207.1158 and
11 online update at <http://www.slac.stanford.edu/xorg/hfag>.

12 [3] M. Antonelli *et al.*, Phys. Rept. **494**, 197 (2010).

13 [4] A. Abulencia *et al.* (CDF Collaboration), Phys. Rev. Lett. **97**, 242003
14 (2006).

15 [5] Rigorously, the mixing phase is the phase of the off-diagonal ele-
16 ment of the mixing transition matrix M_{12} , which approximates $2\beta_s$
17 within $\mathcal{O}(10^{-3})$ corrections. Another often used quantity is $\phi_s \equiv$
18 $\arg[-M_{12}/\Gamma_{12}]$, where Γ_{12} is the decay width of B_s^0 and \bar{B}_s^0
19 mesons into common final states, which governs the asymmetry in B_s^0 semileptonic

- 1 decays of B_s^0 mesons. If significant non-SM contributions affect the mix-
2 ing amplitude, the relation $\phi_s \approx -2\beta_s$ holds among observed quantities.
- 3 [6] I. Dunietz, R. Fleischer, and U. Nierste, Phys. Rev. D **63**, 114015 (2001).
- 4 [7] S. Faller, R. Fleischer, and T. Mannel, Phys. Rev. D **79**, 014005 (2009).
- 5 [8] T. Aaltonen *et al.* (CDF Collaboration), Phys. Rev. Lett. **100**, 161802
6 (2008); V.M Abazov *et al.* (D0 Collaboration), Phys. Rev. Lett. **101**,
7 241801 (2008).
- 8 [9] V.M Abazov *et al.* (D0 Collaboration), Phys. Rev. D **82**, 082001 (2010)
9 and Phys. Rev. D **84**, 052007 (2011).
- 10 [10] T. Aaltonen *et al.* (CDF Collaboration), Phys. Rev. D **85**, 072002
11 (2012).
- 12 [11] V.M Abazov *et al.* (D0 Collaboration), Phys. Rev. D **85**, 032006 (2012).
- 13 [12] R. Aaij *et al.* (LHCb Collaboration), Phys. Rev. Lett. **108**, 101803
14 (2012).
- 15 [13] G. Aad *et al.* (ATLAS Collaboration), arXiv:1208.0572.
- 16 [14] A. Sill *et al.*, Nucl. Instrum. Methods A **447**, 1 (2000); C.S. Hill *et*
17 *al.*, Nucl. Instrum. Methods A **530**, 1 (2004); A. Affolder *et al.*, Nucl.
18 Instrum. Methods A **453**, 84 (2000).
- 19 [15] T. Affolder *et al.*, Nucl. Instrum. Methods A **526**, 249 (2004).

- 1 [16] G. Ascoli *et al.*, Nucl. Instrum. Methods A **268**, 33 (1988).
- 2 [17] D. Acosta *et al.*, Nucl. Instrum. Methods, A **518**, 605 (2004).
- 3 [18] S.M. Berman and M. Jacob, Phys. Rev. **139**, B1023 (1965); I. Dunietz,
4 H. Quinn, A. Snyder, W. Toki, and H.J. Lipkin, Phys. Rev. D **43**, 2193
5 (1991); A.S. Dighe, I. Dunietz, H.J. Lipkin, and J.L. Rosner, Phys. Lett.
6 B **369**, 144 (1996).
- 7 [19] F. Azfar *et al.*, J. High Energy Phys. 1011 (2010) 158.
- 8 [20] S. Leo, Ph. D. Thesis, University of Pisa, Fermilab Report No.
9 FERMILAB-THESIS-2012-14, 2012.
- 10 [21] T. Aaltonen *et al.* (CDF Collaboration), Phys. Rev. Lett. **106**, 121804
11 (2011).
- 12 [22] A. Lenz and U. Nierste, J. High Energy Phys. 0706 (2007) 072, and
13 numerical update in arXiv:1102.4274.
- 14 [23] M. Dorigo, Ph. D. Thesis, University of Trieste, Fermilab Report No.
15 FERMILAB-THESIS-2012-13, 2012.
- 16 [24] B. Aubert *et al.* (BABAR Collaboration), Phys. Rev. D **71**, 032005
17 (2005).
- 18 [25] R. Aaij *et al.* (LHCb Collaboration), Phys. Rev. Lett. **108**, 241801
19 (2012).